

Effect of gain dispersion and stimulated Raman scattering on soliton amplification in fiber amplifiers

Govind P. Agrawal

The Institute of Optics, University of Rochester, Rochester, New York 14627

Received September 17, 1990; accepted November 28, 1990

Amplification of ultrashort solitons in fiber amplifiers is discussed by considering a general model that includes gain saturation, gain dispersion, and intrapulse stimulated Raman scattering. The numerical results show that an interplay between gain dispersion and intrapulse Raman scattering can lead to novel temporal and spectral features. Under high-gain conditions the input pulse is found to split into several subpulses propagating at different speeds. Each subpulse evolves toward a chirped soliton whose width is governed by the gain bandwidth and is ~ 50 fsec for erbium-doped fiber amplifiers.

Recently considerable attention has been focused on the use of erbium-doped fiber amplifiers for soliton amplification because of their potential application in long-distance optical communication systems.¹⁻³ Several authors have studied experimentally⁴⁻⁸ the amplification of ultrashort pulses and have noted that intrapulse stimulated Raman scattering⁹ (ISRS), responsible for the soliton self-frequency shift,^{10,11} appears to play a role. A theoretical understanding of soliton amplification in fiber amplifiers requires the use of a model that includes not only ISRS but also saturation and dispersion of the gain. This Letter presents a general formalism that includes all these effects. The resulting equations are solved numerically to study how ISRS and gain dispersion affect pulse amplification. The results show an initial compression^{12,13} of the fundamental soliton followed by a splitting of the input pulse into several subpulses whose width is determined by the gain bandwidth (generally shorter than 100 fsec). The numerical results are in qualitative agreement with the recent experiments.⁵⁻⁸

For an undoped fiber the effects of ISRS are included by solving a generalized form of the nonlinear Schrödinger equation.^{11,14} The same equation can be used for a fiber amplifier by replacing the fiber loss α by $\alpha - g$, where g is the amplifier gain. In terms of the soliton units this equation takes the form¹⁴

$$i \frac{\partial U}{\partial \xi} + \frac{1}{2} \frac{\partial^2 U}{\partial \tau^2} + N^2 |U|^2 U = N^2 \tau_R \frac{\partial |U|^2}{\partial \tau} U - \frac{i}{2} (\alpha - g) L_D U, \quad (1)$$

where

$$\xi = z/L_D, \quad \tau = (t - z/v_g)/T_0, \quad U = A/P_0^{1/2}, \quad (2)$$

$$N = (\gamma P_0 L_D)^{1/2}, \quad L_D = T_0^2/|\beta_2|, \quad \tau_R = T_R/T_0. \quad (3)$$

Here T_0 and P_0 are the width and the peak power of the input pulse, v_g is the group velocity, β_2 is the group-velocity dispersion parameter ($\beta_2 < 0$ is assumed), γ is

the nonlinearity parameter,¹⁴ and the Raman parameter T_R is related to the slope of the Raman gain profile near the carrier frequency ω_0 ($T_R \simeq 6$ fsec).¹¹ L_D is the dispersion length, and the parameter N is the soliton order ($N = 1$ for the fundamental soliton).

The amplifier gain g in Eq. (1) should generally be obtained by solving the Bloch equations for the dopants (such as erbium) modeled as a pumped two-level system. If the polarization relaxation time T_2 of the gain medium is short enough to satisfy $\Delta\omega T_2 < 1$, where $\Delta\omega$ is the pulse spectral width, coherent effects can be neglected. This is assumed to be the case. The frequency dependence of the gain profile can be approximated by $g(\omega) = g_p[1 - (\omega - \omega_0)^2 T_2^2]$ in the vicinity of the gain peak assumed to be located at the carrier frequency ω_0 . In the time-domain description $\omega - \omega_0$ is replaced by the operator $i(\partial/\partial t)$, and gU in Eq. (1) is given by

$$gU = g_p(\tau) \left(U + \tau_2^2 \frac{\partial^2 U}{\partial \tau^2} \right), \quad (4)$$

where $\tau_2 = T_2/T_0$ is the gain-dispersion parameter. The time dependence of the peak gain results from gain saturation and is obtained by solving

$$\frac{\partial g_p}{\partial \tau} = \frac{g_0 - g_p}{T_1/T_0} - \frac{g_p P_0 T_0}{E_s} |U|^2, \quad (5)$$

where g_0 is the unsaturated (small-signal) gain, T_1 is the population decay time ($T_1 \sim 1$ msec), $E_s = \hbar\omega_0 A_{\text{eff}}/\sigma$ is the saturation energy, σ is the transition cross section, and A_{eff} is the effective core area of the fiber. Typically $E_s \sim 1 \mu\text{J}$ for fiber amplifiers. In most cases of practical interest $T_1/T_0 \gg 1$, and the T_1 term can be neglected in Eq. (5) during pulse amplification. Equation (5) is then easily solved to yield

$$g_p(\tau) = g_0 \exp\left(-s \int_{-\infty}^{\tau} |U|^2 d\tau\right), \quad (6)$$

where $s = P_0 T_0/E_s$ is the saturation parameter. For a fundamental soliton, $s \sim 10^{-5}$, and gain saturation is negligible during the amplification of a single pulse;

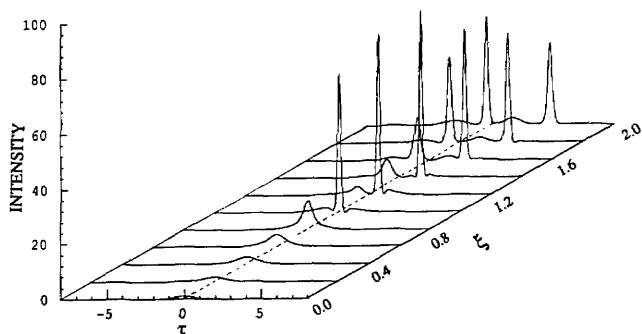


Fig. 1. Evolution of a fundamental soliton over two dispersion lengths inside a fiber amplifier with gain of 10 dB per dispersion length. The other parameters are $s = 10^{-5}$, $\tau_2 = 0.2$, and $\tau_R = 0.02$.

for a pulse train g_0 may differ from pulse to pulse if the repetition rate $R \gg 1/T_1$. By substituting Eqs. (4) and (6) into Eq. (1), we obtain

$$i \frac{\partial U}{\partial \xi} + \frac{1}{2} \frac{\partial^2 U}{\partial \tau^2} + N^2 |U|^2 U = N^2 \tau_R \frac{\partial |U|^2}{\partial \tau} U - i \frac{\alpha}{2} L_D U + \frac{i}{2} g_0 L_D \exp\left(-s \int_{-\infty}^{\tau} |U|^2 d\tau\right) \left(U + \tau_2^2 \frac{\partial^2 U}{\partial \tau^2}\right). \quad (7)$$

This equation includes gain saturation through the parameter s , gain dispersion through the parameter τ_2 , and ISRS through the parameter τ_R . For $T_0 = 0.3$ psec, it is estimated that $s \approx 10^{-5}$, $\tau_2 = 0.2$, and $\tau_R = 0.02$, and these parameter values are used for the numerical results. Equation (7) can be further generalized to include the effects of higher-order dispersion and self-steepening¹⁴; their effect is, however, negligible on the results presented here.

To study the amplification of fundamental solitons in fiber amplifiers, Eq. (7) is solved numerically for $N = 1$ with the initial amplitude $U(0, \tau) = \text{sech } \tau$ by using the split-step Fourier method.¹⁴ Figure 1 shows the evolution of a soliton in the range $\xi = 0-2$ for an amplifier gain of 10 dB per dispersion length. In the range $\xi = 0-1$ the most noteworthy feature of Fig. 1 is the pulse compression¹¹; the pulse width is reduced by approximately a factor of 10 at $\xi = 1$ from its initial value without a significant pedestal. Such a width reduction is of considerable practical importance as it can be used to amplify and compress femtosecond pulses simultaneously. Beyond $\xi = 1$ the pulse shifts to the right side, and a new pulse begins to form. The shift is due to ISRS and results from a transfer of pulse energy toward low-frequency components that travel slower than the original pulse in the anomalous-dispersion regime of the fiber. Figure 2 shows the pulse spectra in the range $\xi = 0-1.4$. Considerable spectral broadening occurs beyond $\xi = 0.8$. The spectra become asymmetric with multiple peaks and indicate that the pulse is considerably chirped.

Figure 3 compares the pulse spectrum and the frequency chirp for $\xi = 1$ and 2. The pulse spectrum changes considerably between $\xi = 1$ and 2. Two qualitatively new features are the suppression of the soliton self-frequency shift and the splitting of the pulse spectrum into several spectral bands. Both of these fea-

tures are due to the simultaneous presence of ISRS and gain dispersion. Blow *et al.*¹⁵ have shown that bandwidth-limited amplification of ultrashort pulses can suppress the self-frequency shift induced by ISRS. Spectral splitting beyond $\xi = 1.4$ (seen in Fig. 3 at $\xi = 2$) appears to be related to the twin-pulse temporal profile seen in Fig. 1. The physical origin of the appearance of two pulses can be traced to the chirped solitary-wave solution of Eq. (7) obtained by Bélanger *et al.*¹³ for the case of $\tau_R = 0$ and $s = 0$. Both the width and the energy of such a soliton are determined by $T_2/\sqrt{3}$ for the parameter values used in Figs. 1-3. In the absence of ISRS the input soliton evolves toward such a chirped soliton asymptotically.¹⁶ ISRS slows down this soliton because of a small spectral shift. This is the reason for the shift of the main peak toward the right in Fig. 1. A second peak begins to develop be-

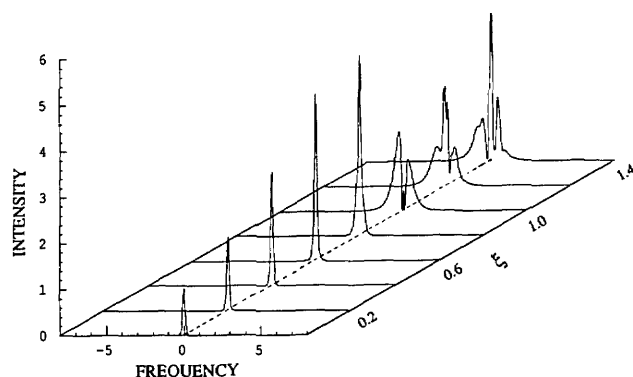


Fig. 2. Evolution of pulse spectra corresponding to the pulse shapes shown in Fig. 1.

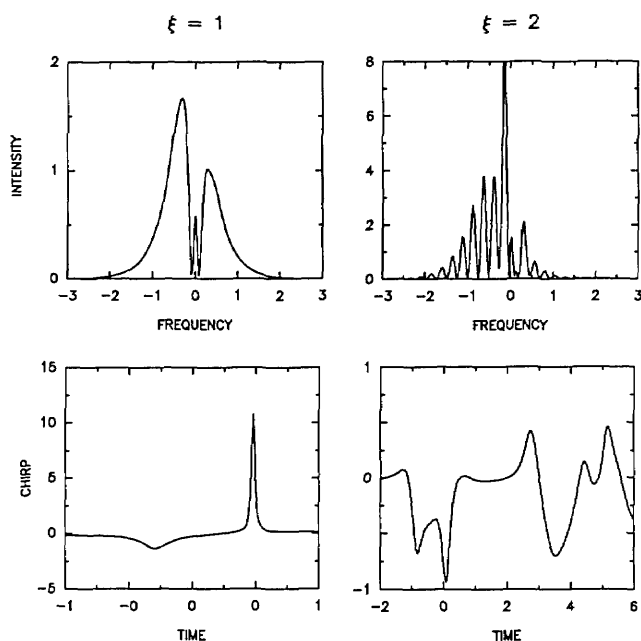


Fig. 3. Pulse spectra (upper row) and chirp profiles (lower row) at $\xi = 1$ (left-hand column) and $\xi = 2$ (right-hand column). The corresponding pulse shapes are shown in Fig. 1.

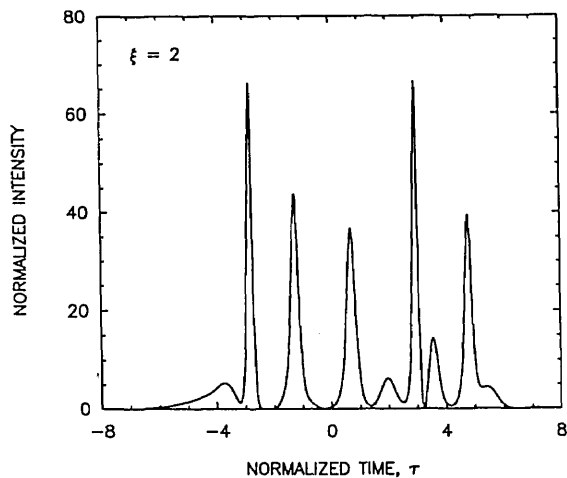


Fig. 4. Pulse shape at $\xi = 2$ for a fiber amplifier with a gain of 20 dB per dispersion length. The other parameters are the same as those in Fig. 1.

yond $\xi = 1$ and is amplified by the fiber amplifier since its spectrum is located near the gain peak. This peak also appears to evolve toward a chirped soliton. Spectral splitting seen in Fig. 3 can be interpreted as an interference pattern between the two chirped solitary pulses. Eventually a third soliton forms as the input pulse propagates beyond $\xi = 2$.

When the amplifier gain is relatively large, pulse splitting begins to occur for shorter propagation distances. The temporal profile in that case can consist of multiple ultrashort pulses of different widths and peak intensities. Figure 4 shows such a profile at $\xi = 2$ for the case in which the amplifier gain is 20 dB per dispersion length. A multiple-pulse pattern is also found to occur in the absence of ISRS,¹⁶ which indicates that gain dispersion is responsible for such a structure. However, the temporal profile is symmetric with nearly equal amplitudes for various subpulses when $\tau_R = 0$. The asymmetry seen in Fig. 4 is due solely to ISRS. The main point is that an interplay between the effects of gain dispersion and ISRS can lead to novel spectral and temporal features.

Some of the features of soliton amplification discussed above have been observed in the recent experiments on erbium-doped fiber amplifiers with femtosecond pulses.⁶⁻⁸ Pulse compression by as much as a factor of 4 has been seen by using 260-fsec pulses.⁸ In an interesting experiment⁶ with a net gain of 21.5 dB the autocorrelation trace of the output pulse indicated splitting of the 180-fsec input pulse into at least five separate pulses, a behavior qualitatively similar to that shown in Fig. 4. In another experiment⁷ 120-fsec input pulses were found to form a 55-60-fsec pulse in the Stokes wing whose width did not change significantly with the fiber length. This behavior is similar to that shown in Fig. 1 and suggests that a chirped soliton was observed in this experiment. The simula-

tions indicate that this soliton has its origin in gain dispersion¹³ rather than in ISRS. The role of ISRS is to shift the spectrum and delay the soliton. A multi-peak spectrum similar to those seen in Fig. 2 has also been observed.⁸

In conclusion, amplification of ultrashort solitons in fiber amplifiers is discussed by considering a general model that is capable of including gain saturation, gain dispersion, and ISRS. The results show that an interplay between gain dispersion and ISRS can lead to novel temporal and spectral features. For a relatively low amplifier gain the input pulse is simultaneously amplified and compressed; the width of the compressed pulse is determined by T_2 and is expected to be ~ 50 fsec for erbium-doped fiber amplifiers. Under high-gain conditions the input pulse splits into many subpulses, each of which evolves toward a chirped soliton of width $\approx T_2/\sqrt{3}$. The numerical results are in qualitative agreement with recent experiments.⁴⁻⁸

This research is partially supported by the National Science Foundation, the U.S. Army Research Office, and the New York State Science and Technology Foundation.

References

1. M. Nakazawa, K. Suzuki, and Y. Kimura, *IEEE Photon. Technol. Lett.* **2**, 216 (1990).
2. K. Iwatsuki, S. Nishi, and K. Nakagawa, *IEEE Photon. Technol. Lett.* **2**, 355 (1990).
3. N. A. Olsson, P. A. Andrekson, P. C. Becker, J. R. Simpson, T. Tanbun-Ek, R. A. Logan, H. Presby, and K. Wecht, *IEEE Photon. Technol. Lett.* **2**, 358 (1990).
4. A. Takada, K. Iwatsuki, and M. Saruwatari, *IEEE Photon. Technol. Lett.* **2**, 122 (1990).
5. B. J. Ainslie, K. J. Blow, A. S. Gouveia-Neto, P. G. J. Wigley, A. S. B. Sombra, and J. R. Taylor, *Electron. Lett.* **26**, 186 (1990).
6. I. Yu. Khrushchev, A. B. Grudinin, E. M. Dianov, D. V. Korobkin, V. A. Semenov, and A. M. Prokhorov, *Electron. Lett.* **26**, 456 (1990).
7. A. B. Grudinin, E. M. Dianov, D. V. Korobkin, A. Yu. Makarenko, A. M. Prokhorov, and I. Yu. Khrushchev, *JETP Lett.* **51**, 135 (1990).
8. M. Nakazawa, K. Kurokawa, H. Kubota, K. Suzuki, and Y. Kimura, *Appl. Phys. Lett.* **57**, 653 (1990).
9. E. M. Dianov, A. Ya. Karasik, P. B. Mamyshev, A. M. Prokhorov, V. N. Serkin, M. F. Stelmakh, and A. A. Fomichev, *JETP Lett.* **41**, 294 (1985).
10. F. M. Mitschke and L. F. Mollenauer, *Opt. Lett.* **11**, 659 (1986).
11. J. P. Gordon, *Opt. Lett.* **11**, 662 (1986).
12. K. J. Blow, N. J. Doran, and D. Wood, *J. Opt. Soc. Am. B* **5**, 381 (1988).
13. P. A. Bélanger, L. Gagnon, and C. Paré, *Opt. Lett.* **14**, 943 (1989).
14. G. P. Agrawal, *Nonlinear Fiber Optics* (Academic, Boston, Mass., 1989), Chap. 5.
15. K. J. Blow, N. J. Doran, and D. Wood, *J. Opt. Soc. Am. B* **5**, 1301 (1988).
16. G. P. Agrawal, *IEEE Photon. Technol. Lett.* **2**, 875 (1990).